Quantifying the Effects of Quadrupolar Sink via ^{15}N Relaxation Dynamics in Metronidazoles Hyperpolarized via SABRE-SHEATH

Jonathan R. Birchall[1], Mohammad S. H. Kabir[1], Oleg G. Salnikov[2,3,4], Nikita V. Chukanov[2,3], Alexandra Svyatova[2,3], Kirill V. Kovtunov[2,3], Igor V. Koptyug[2,3], Juri G. Gelovani[1,5], Boyd M. Goodson[6], Wellington Pham[7], and Eduard Y. Chekmenev[1,8]

[1]Department of Chemistry, Ibio, Wayne State University, Karmanos Cancer Institute (KCI), Detroit, MI, USA
[2]International Tomography Center, [3]Novosibirsk State University, [4]Boreskov Institute of Catalysis, Novosibirsk, Russia
[5]United Arab Emirates University, Al Ain, United Arab Emirates
[6]Department of Chemistry and Biochemistry, Southern Illinois University, Carbondale, IL, USA
[7]Vanderbilt University Institute of Imaging Science (VUIIS), Nashville, Tennessee, United States
[8]Russian Academy of Sciences, Leninskiy Prospekt 14, Moscow, Russia

WAYNE STATE UNIVERSITY

ABSTRACT

Spin-lattice relaxation dynamics of ^{15}N nuclei in metronidazole-$^{15}N_3$ and metronidazole-$^{15}N_2$ isotopologues are studied in the context of developing strategies for rational design of ^{15}N enriched biomolecules for Signal Amplification by Reversible Exchange (SABRE) in microtesla magnetic fields. In this process, parahydrogen and the to-be-hyperpolarized substrate undergo simultaneous reversible chemical exchange on an iridium complex; nuclear spin polarization from parahydrogen derived hydrides is then spontaneously transferred among ^{15}N nuclei within each metronidazole isotopologue via a network that includes two-bond ^{15}N-^{15}N spin-spin couplings. Quantitative mapping of ^{15}N relaxation dynamics reveals the deleterious effects of interactions with polarization transfer catalyst (containing quadrupolar Ir nucleus) and quadrupolar ^{14}N nucleus within the spin-relayed network. Although the catalyst decreases the ^{15}N spin-relaxation time constant, T_1, of metronidazole isotopologues in the microtesla regime in a concentration-dependent manner, the overall impact on the achievable ^{15}N polarization level is relatively minor. On the other hand, the presence of a ^{14}N nucleus in the scalar coupling network results in an approximately 3-fold decrease of microtesla ^{15}N T_1 values for all ^{15}N sites in the $^{15}N_2$-isotopologue versus the $^{15}N_3$-isotopologue over a wide range of catalyst concentrations. This ^{15}N T_1 reduction results in a corresponding 3-fold decrease of ^{15}N polarization levels. These findings have substantial translational relevance for the rational design of hyperpolarized MRI contrast agents comprising ^{15}N and ^{13}C labeled biomolecules both in general, and in the specific case of SABRE-hyperpolarized metronidazole, an antibiotic that can be potentially employed for non-invasive hypoxia sensing.

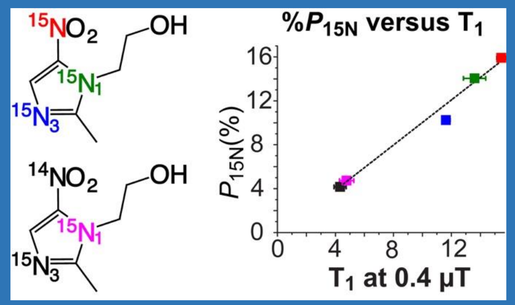

REFERENCES

1. Birchall JR, Kabir MSH, Salnikov OG, Chukanov NV, Svyatova A, Kovtunov KV, Koptyug IV, Gelovani JG, Goodson BM, Pham W, Chekmenev EY. Quantifying the effects of quadrupolar sinks via ^{15}N relaxation dynamics in metronidazoles hyperpolarized via SABRE-SHEATH. Chemical Communications. 2020
2. Shchepin RV, Birchall JR, Chukanov NV, Kovtunov KV, Koptyug IV, Theis T, Warren WS, Gelovani JG, Goodson BM, Shokouhi S, Rosen MS. Hyperpolarizing Concentrated Metronidazole $^{15}NO_2$ Group over Six Chemical Bonds with More than 15% Polarization and a 20 Minute Lifetime. Chemistry–A European Journal. 2019 Jul 2;25(37):8829-36
3. Adams RW, Aguilar JA, Atkinson KD, Cowley MJ, Elliott PI, Duckett SB, Green GG, Khazal IG, López-Serrano J, Williamson DC. Reversible interactions with para-hydrogen enhance NMR sensitivity by polarization transfer. Science. 2009 Mar 27;323(5922):1708-11
4. Shchepin RV, Jaigirdar L, Theis T, Warren WS, Goodson BM, Chekmenev EY. Spin relays enable efficient long-range heteronuclear signal amplification by reversible exchange. The Journal of Physical Chemistry C. 2017 Dec 28;121(51):28425-34
5. Barskiy DA, Pravdivtsev AN, Ivanov KL, Kovtunov KV, Koptyug IV. A simple analytical model for signal amplification by reversible exchange (SABRE) process. Physical Chemistry Chemical Physics. 2016;18(1):89-93.

ABOUT CHEKMENEV LAB

Chekmenev group develops hyperpolarized magnetic resonance (MR). The technique of hyperpolarization enhances nuclear spin polarization by 4-6 orders of magnitude with the corresponding gains in MRI detection sensitivity. As a result, it becomes possible to image dilute compounds such as metabolites and functional contrast agents reporting on in cellular metabolism and organ function respectively. The focus of Chekmenev work is on low-cost and high-throughput hyperpolarization approaches such as PHIP, SABRE, and SEOP. The produced contrast agent (hyperpolarized ^{129}Xe) can be inhaled for functional 3D MRI scan of lung ventilation and gas diffusion on a single patient breath hold. With SABRE technology, we have been focusing on development molecular probes to report on abnormal metabolism (pH, hypoxia and others) in cancer and other diseases.

INTRODUCTION

Signal Amplification by Reversible Exchange (SABRE), pioneered by Duckett *et al*. in 2009, which utilizes simultaneous reversible chemical exchange of parahydrogen (*p*-H2) and to-be-hyperpolarized substrate molecules at a metal center. In SABRE, the transfer of nuclear spin polarization from parahydrogen-derived hydrides to a spin-polarizable substrate occurs spontaneously via the network of spin–spin couplings established in a transient polarization transfer catalyst (PTC) complex (Fig. 1a). Here we used SABRE-SHEATH, as it is performed at very low magnetic fields (<1 μT) and near room temperature, the production of such HP ^{15}N spin-labeled biomolecules is comparatively simple, fast and inexpensive. Metronidazole is an FDA-approved antibiotic, belonging to the nitroimidazole class of compounds. We envision that ^{15}N-hyperpolarized metronidazole can be potentially employed for hypoxia sensing in a manner similar to that of nitroimidazole-based PET tracers. One such tracer, ^{18}F-fluoromisonidazole (FMISO), undergoes reduction in hypoxic environment (including most notably hypoxic tumors) and the metabolic products of this reduction process become trapped in hypoxic cells, providing contrast in FMISO PET images. The enormous potential for using HP MRI to sense metabolic transformations *in vivo* has been well demonstrated; correspondingly, HP MRI of metronidazole may obviate the limitations of FMISO PET imaging, including the use of ionizing radiation, the requirement for long clearance time from surrounding tissues, and the inability to spectrally distinguish parent compounds from downstream products. Here, we report a quantitative study of spin relaxation dynamics of metronidazole-$^{15}N_2$ and metronidazole-$^{15}N_3$ isotopologues.

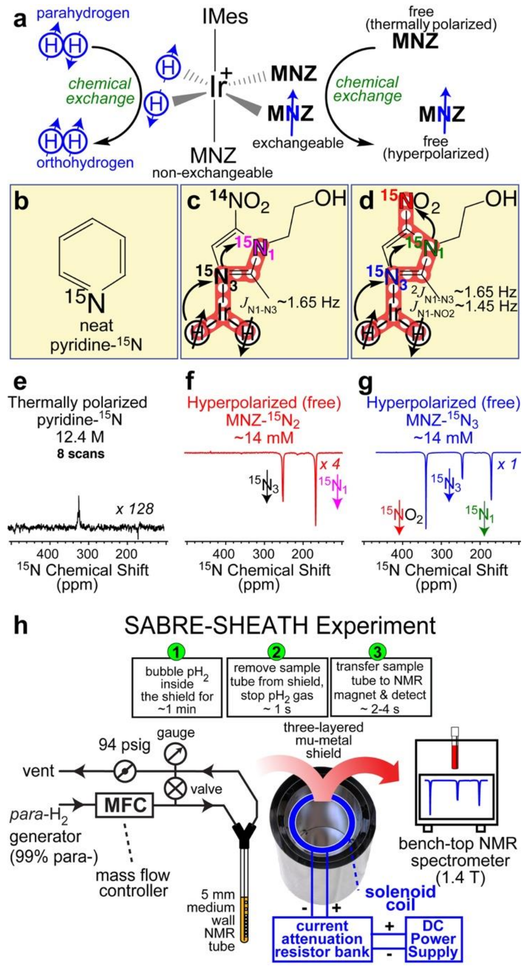

Figure 1. a) Molecular exchange between p-H_2 and metronidazole (MNZ) b) Structure of pyridine-^{15}N c-d) Corresponding structures and polarization transfer spin-relays (red overlay) between *p*-H_2 and ^{15}N nuclei in corresponding MNZ ^{15}N-isotopologues. e) Thermally polarized neat pyridine-^{15}N f-g) Corresponding ^{15}N NMR spectra of HP metronidazole-$^{15}N_2$ and metronidazole-$^{15}N_3$. h) Experimental setup of SABRE-SHEATH.

RESULTS

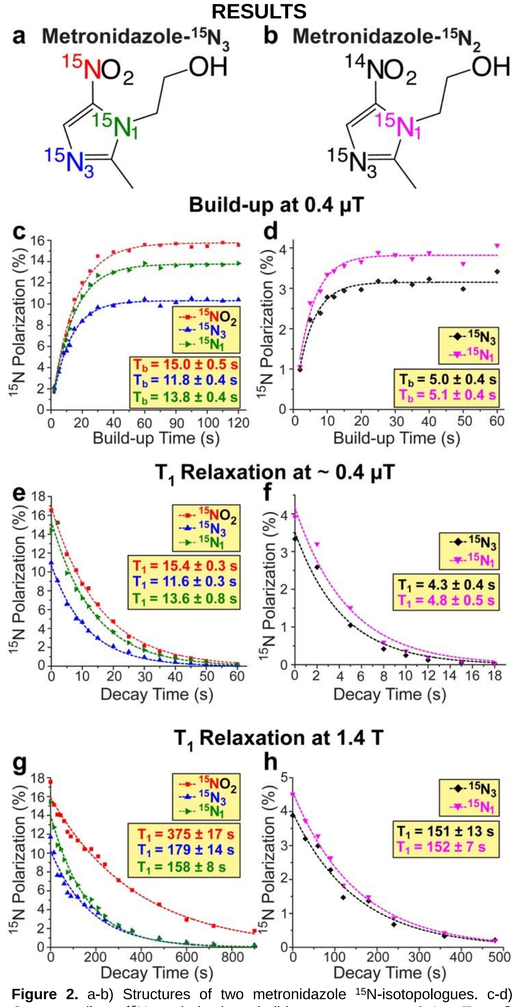

Figure 2. a-b) Structures of two metronidazole ^{15}N-isotopologues. c-d) Corresponding ^{15}N polarization build-up curves at 0.4 μT. e-f) Corresponding ^{15}N T_1 decay curves at 0.4 μT. g-h) Corresponding ^{15}N T_1 decay curves at 1.4 T. The presented data was recorded using a 2 mM IrIMes catalyst concentration and a corresponding 20 mM MNZ isotopologue concentration.

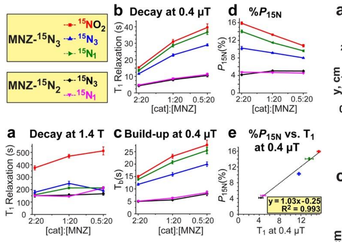

Figure 3. a) Dependence of ^{15}N polarization T_1 decay at 1.4 T on the catalyst-to-substrate concentration ratio. b) Same as (a), but at 0.4 mT. c) Dependence of ^{15}N polarization build-up time constant (T_b) at 0.4 μT on the catalyst-to-substrate concentration ratio. d) Dependence of ^{15}N steady-state polarization value (achieved after 1 min. of build-up) on the catalyst-to-substrate concentration ratio. e) Dependence of %P_{15N} on ^{15}N T_1 at 0.4 μT, using 2 mM IrIMes catalyst concentration and 20 mM MNZ-$^{15}N_3$ or MNZ-$^{15}N_2$.

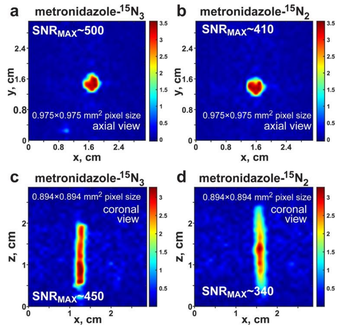

Figure 4. ^{15}N MRI of 5 mm NMR tubes filled with hyperpolarized solutions of 0.1 M metronidazole-$^{15}N_3$ (MNZ-$^{15}N_3$) and metronidazole-$^{15}N_2$ (MNZ-$^{15}N_2$) using 5 mM of Ir(COD)(IMes)Cl in methanol-d_4 obtained by TrueFISP pulse sequence.

DISCUSSION

The key results related to ^{15}N T_1 relaxation at the optimal magnetic field during the SABRE-SHEATH polarization transfer process (ca. 0.4 μT, Figure 5) for metronidazole-$^{15}N_3$ and metronidazole-$^{15}N_2$ are shown in Figures 2e and 2f, respectively. As expected for microtesla magnetic fields, all ^{15}N sites within a given molecule share approximately the same relaxation rate (e.g., 13.8-15.4 s for MNZ-$^{15}N_3$, Figure 2e). However, the $^{15}NO_2$ group replacement by $^{14}NO_2$ leads to dramatic, 3-fold shortening of the ^{15}N T_1 (4.3-4.8 s corresponding T_1 values for MNZ-$^{15}N_2$, Figure 2f). This striking effect can be explained by the enhanced scalar relaxation of the second kind induced by the quadrupolar $^{14}NO_2$ site within the N-N spin-spin coupling network.

These results are further supported by the overall similar ^{15}N T_1 trend at the Earth's magnetic field (ca. 10 μT in the basement of our lab at Detroit, MI, Table 1). Moreover, we find that each ^{15}N polarization build-up constant (T_b, Figure 2c and Figure 2d) at 0.4 μT is closely correlated with the corresponding T_1 value. In practice, this means that the increased relaxation rate caused by the presence of the quadrupolar ^{14}N spin in MNZ-$^{15}N_2$ (despite the peripheral position of the NO_2 group) allows for achieving the steady-state %P_{15N} faster on $^{15}N_3$ and $^{15}N_1$ sites, but at significantly lower levels. The correlation plot of %P_{15N} versus T_1 at 0.4 μT indeed exhibits a linear trend with R^2>0.99 (Figure 3e). When the magnetic field is sufficiently high (e.g., 1.4 T, Figure 2g and Figure 2h), the increased frequency dispersion of the nuclear spins puts them in a weakly coupled regime with ^{15}N sites having significantly longer T_1 decay constants-on the order of many minutes.

It should be pointed out that substrate exchange of Ir-IMes catalyst may act as the potential source of additional undesirable ^{15}N relaxation (e.g., due to compounding effects of quadrupolar Ir nucleus and the chemical exchange process). Consequently, a series of control experiments were performed, where the catalyst concentration was systematically varied from 0.5 mM to 1 mM to 2 mM at a fixed concentration of metronidazole isotopologue (Figures 3a-d). The [catalyst] increase from 0.5 mM to 2 mM results in a stepwise decrease in ^{15}N T_1 and T_b by approximately 2-fold at 0.4 μT (Figure 3b and Figure 3c). However, because the interplay of T_1 relaxation and catalyst concentration is complex in the SABRE process, these decreases in ^{15}N T_1 and T_b at 0.4 μT are offset by the overall increased catalyst-to-substrate ratio (i.e., better substrate access to *p*-H_2 spin bath), resulting in somewhat greater %P_{15N} in metronidazole-$^{15}N_3$ and similar %P_{15N} in metronidazole-$^{15}N_2$ at higher [catalyst], Figure 3d. Of note, the Ir-IMes catalyst decreases ^{15}N T_1 even at high magnetic fields (1.4 T, weakly coupled regime) for $^{15}NO_2$ (Figure 3a). Moreover, this observation clearly indicates a second reason (beyond agent purification) that SABRE catalyst removal is warranted as soon polarization build-up is completed to minimize ^{15}N polarization losses prior to biomedical utilization of HP metronidazole-$^{15}N_3$ as a contrast agent.

On another note, the realization that scalar-coupled ^{14}N spins are highly deleterious in the context of SABRE-SHEATH suggests that if these quadrupolar effects would have been avoided, near-unity P_{15N} would have been potentially achievable in the previous studies.

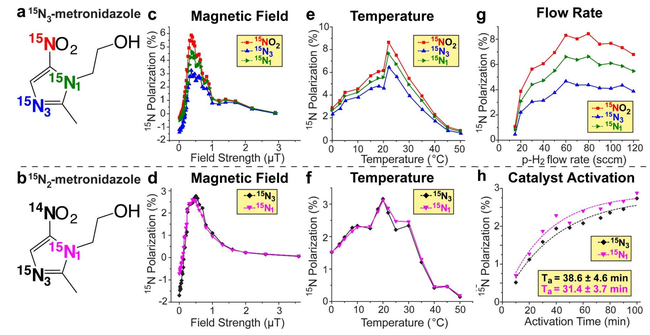

Figure 5. Optimization of experimental parameters at 2 mM IrIMes catalyst with 20 mM of MNZ-$^{15}N_2$ VS MNZ-$^{15}N_3$

ACKNOWLEDGEMENTS

NSF CHE-1904780 and CHE-1905341, NIH R21CA220137, DOD CDMRP W81XWH-12-1-0159/BC112431, W81XWH-15-1-0271 and W81XWH-15-1-0272. O.G.S. thanks the RFBR #19-33-60045 for the support of mechanistic studies with the use of p-H2. N.V.C. and K.V.K. thank the Russian Science Foundation #17-73-20030 for their support in the synthesis of ^{15}N-labeled compounds. I.V.K. thanks the Russian Ministry of Science and Higher Education (project AAAA-A16-116121510087-5) and the RFBR (grants 19-29-10003, 17-54-33037) for financial support.